*J Toxicol Pathol 2009; **22**: 173–178*

Original

Malignant Lymphoma with Severe Infiltrative Growth into Skeletal Muscles in WBN/Kob Rats

Tomoya Sano[1], Kiyokazu Ozaki[1], Yasushi Kodama[2], Tetsuro Matsuura[1], and Isao Narama[1]

[1]Department of Pathology, Faculty of Pharmaceutical Sciences, Setsunan University, 45–1 Nagaotoge-cho, Hirakata City, Osaka 573-0101, Japan
[2]Laboratory of Molecular and Cellular Toxicology, Faculty of Pharmaceutical Sciences, Hiroshima International University, 5–1–1 Hirokoshingai, Kure City, Hiroshima 737-0112, Japan

Abstract: Although spontaneously occurring neoplasms have been reported repeatedly in F344, SD and Wistar rats, which are commonly used strains for routine toxicologic and carcinogenicity studies, there are only a few reports of malignant lymphoma or lymphatic leukemia except for large granular lymphocytic leukemia (LGL) in F344 rats. Malignant lymphoma (lymphosarcoma) is thought to be uncommon in F344 rats. The authors encountered malignant lymphomas of the non-LGL leukemia type with characteristic pathologic features in WBN/Kob rats. The mean age at onset of the disease in all 13 affected rats (8 males and 5 females) was about 60 weeks. Common and characteristic clinical signs were abnormal gait with hind limb paralysis. Macroscopically, the enlargement of the lymph nodes, spleen and liver was slight to moderate. Scattered multiple white-to-gray nodules encompassed the aorta and assumed a bead-like appearance near the thoracic and lumbar vertebrae. Histopathologically, neoplastic proliferative changes were predominant in the bone marrow tissue of the entire body, and many tumor cells infiltrated the spleen and several lymph nodes. The most striking histological features were constant and severe infiltration of tumor cells in the adipose tissue and skeletal muscle adjacent the thoracic and lumber vertebrae. Immunohistochemically, all tumor cells were positive for B-cell markers (PAX-5, CD79a and CD45) and negative for CD3. From the results of immunohistochemistry and morphological examination, these tumors were diagnosed as malignant B-cell lymphomas. (J Toxicol Pathol 2009; **22**: 173–178)

Key words: malignant lymphoma, B cell, WBN/Kob rat

Introduction

Various kinds of spontaneously occurring neoplasms have often been reported in F344, SD and Wistar rats along with other incidental findings as background data, because these rat strains have been commonly used for routine toxicologic and carcinogenicity studies for various chemicals including drugs. However, spontaneous lymphoma and leukemia are considered to be less common diseases in the rat compared with the mouse. Lymphoma has been reported in several strains of rats including Long-Evans, Wistar-Furth, Wistar and Sprague-Dawley[1–7]. Most of the previous studies have reported malignant lymphomas generally observed in aged rats[4–7]. Only a few reports of malignant lymphoma or lymphatic leukemia have been published except for large granular lymphocyte (LGL) leukemia in F344 rats[8,9]. Cytological and immunohistological classification of murine lymphoma has been proposed by several researchers, and a strain-specific predilection for some types of lymphoma or leukemia was recognized in some strains, such as LGL leukemia in F344 rats. Malignant lymphoma (lymphosarcoma) other than LGL leukemia is thought to be rather uncommon in F344 rats[8,9].

WBN/Kob rats are an inbred strain of Wistar rats established as diabetic model animals that spontaneously develop long-lasting diabetic symptoms[10,11] and various diabetic complications in aged males[12–16]. We observed uncommon-type malignant lymphomas (leukemia) of the non-LGL leukemia type with characteristic pathologic features in this strain of rats maintained in our laboratory. To clarify the morphological and cytological characteristics of this type of lymphoma, the clinical course, histopathological and immunocytochemical features of the affected animals were examined.

Received: 24 April 2009, Accepted: 18 May 2009
Mailing address: Isao Narama, Department of Pathology, Faculty of Pharmaceutical Sciences, Setsunan University, 45–1 Nagaotoge-cho, Hirakata City, Osaka 573-0101, Japan
TEL: 81-72-866-3162 FAX: 81-72-866-32491
E-mail: narama@pharm.setsunan.ac.jp

Materials and Methods

Animals

Male and female WBN/Kob rats were obtained from the Shizuoka Laboratory Animal Center (Shizuoka, Japan) and maintained for over a decade in our laboratory. They were reared in a barrier-sustained animal room maintained at a temperature of 24 ± 2°C and a relative humidity of 60 ± 20% with 12-h light/dark cycles, and ventilated at least 12 times/h with sterilized fresh air. All rats were housed and reared in aluminum mesh cages. The cages were changed at least once every week. The rats were given a pellet diet (CRF-1; Oriental Yeast, Tokyo, Japan) and chlorinated water *ad libitum*.

All procedures for animal handling and experimental treatments were in accordance with the Guidelines for the Care and Use of Laboratory Animals of the Committee for Animal Experiments of Setsunan University and the Japanese Association for Laboratory Animal Science. The level of care provided to the animals met the basic requirements outlined in the National Institutes of Health guidelines (Humane endpoints for animals used in biomedical research and testing, ILAR Journal Vol 41(2) 2000; National Institute of Health Guide For the Care and Use of Laboratory Animals, NIH Publication 1996).

The average age of the 8 male and 5 female affected WBN/Kob rats was about 60 (ranged 35 to 106) weeks at the onset of the disease. Blood smears for microscopic observation of peripheral leukocytes were made for three rats. All rats were necropsied and underwent a full pathologic examination immediately after being sacrificed by CO_2 inhalation.

Histopathological analysis

Organs and tissues were enucleated immediately after necropsy and immersed in 10% neutral buffered formalin solution. The fixed organs were trimmed, dehydrated by an automated processor, and embedded in paraffin. Sections (4-μm thick) of tissue specimens were stained with hematoxylin-eosin for histopathological examination.

Immunohistochemical analysis

Immunohistochemical analysis of tumor cells was performed using antibodies to the T-cell cell-surface antigen CD3 and B-cell markers CD79α, CD45RA and PAX-5 in lymph node sections. These sections were deparaffinized in xylene, and rehydrated through graded ethanol at room temperature. Rehydrated sections were digested by pepsin for 20 min at 37°C to retrieve antigen. Solutions were prepared using 0.05 M Tris buffered saline (TBS, pH 7.6) with 0.01% Tween 20, and these media were also used for washes between the various steps. Non-specific endogenous peroxidase activity was blocked by exposure to 0.03% hydrogen peroxide in 100% methanol for 5 min, and masking was conducted with 1% bovine serum albumin or 5% normal goat serum in phosphate-buffered saline for 5 min at room temperature. Incubation was carried out overnight at 4°C with primary antibodies, such as anti-CD3 (diluted 1:100, Dako, Japan), CD79αcy (diluted 1:40, Dako, Japan), CD45RA (diluted 1:400, AbD Serotec, UK) and Pax5 (diluted 1:10, Abcam, UK) monoclonal antibodies. The slides were subsequently rinsed with TBS plus Tween 20, treated for 30 min at room temperature with Histofine Simple Stain Rat MAX PO (M) (Nichirei, Japan), rinsed with TBS plus Tween 20, incubated in diaminobenzidine solution containing 0.01% hydrogen peroxide for the peroxidase coloring reaction, and counterstained with Mayer's hematoxylin.

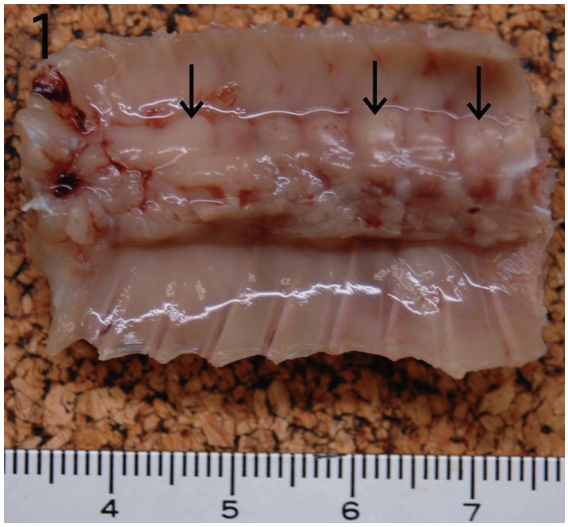

Fig. 1. Scattered multiple white-to-gray nodules (arrow) encompassing the aorta assume a bead-like appearance near the thoracic vertebra.

Results

Clinical signs and macroscopic findings

Common and characteristic clinical signs included abnormal gait with paralysis of the hind limb. Excessive avoiding behavior was often observed before the appearance of abnormal gait when the rats were touched or the posterior parts of the body were held. The affected rats wasted rapidly after the appearance of clinical signs and became moribund within a few days.

In two out of 13 rats, moderate to severe enlargement of the spleen and liver with mild enlargement of many lymph nodes were the most striking necropsy findings. The size of the spleen was 9 × 2 × 2 cm (about 3 to 5 times the spleen of an age-matched normal male rat of this strain) in the most severely enlarged male case. The liver of this rat was tan in color and was also enlarged, 9 × 7 × 2 cm (about 1.5 to 2 times of the liver of age-matched normal male), but the enlargement was less severe than that of the spleen. Enlargement of the spleen and liver was slight or inconspicuous in the other cases.

The most conspicuous and characteristic macroscopic changes in the majority of the affected rats were scattered

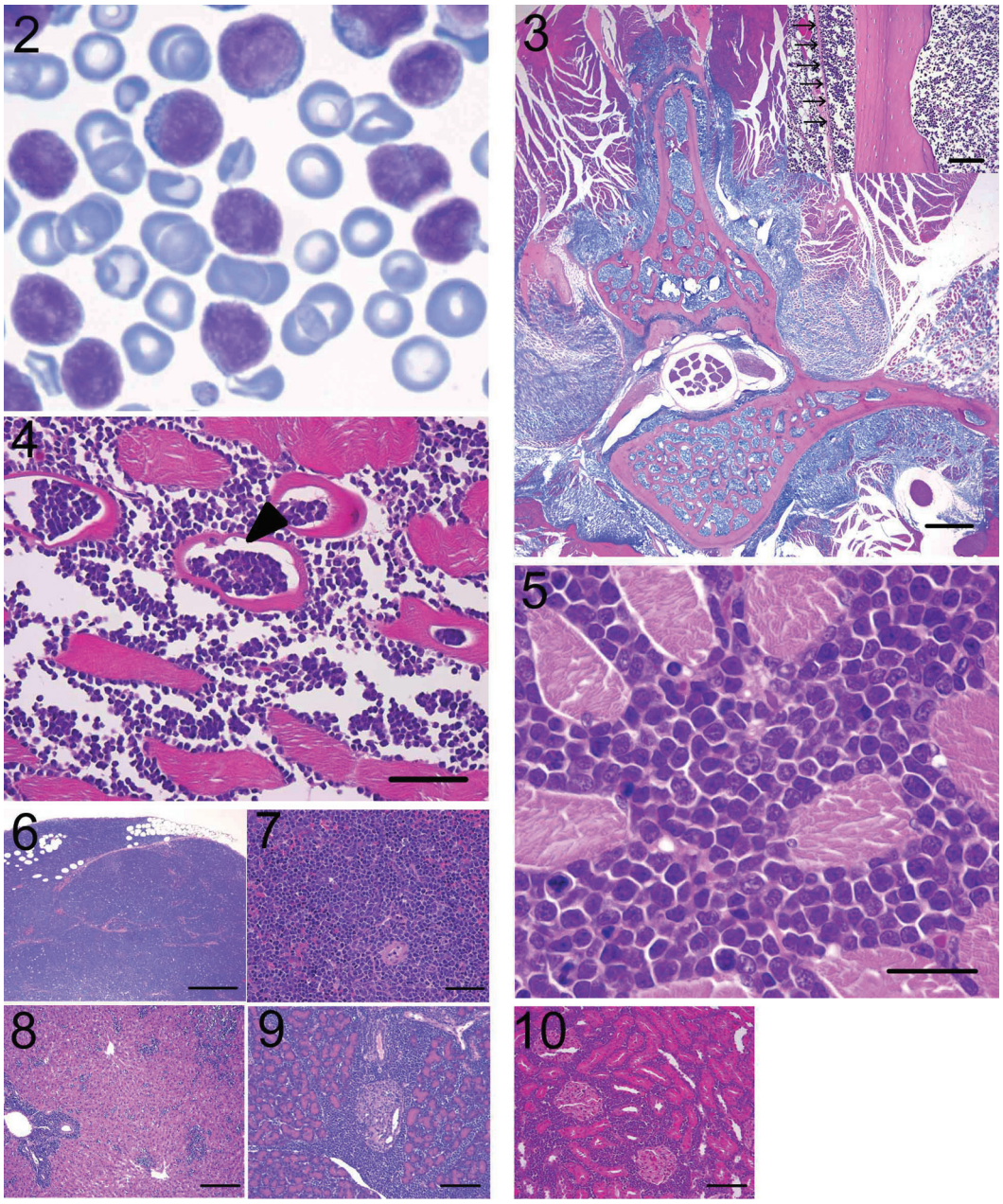

Fig. 2. Tumor cells have scanty basophilic cytoplasm, cleaved round nuclei with aggregated chromatin and prominent nucleoli.
Fig. 3. Tumor cells severely infiltrated the bone marrow, periosteum, adipose tissue and skeletal muscles adjacent to lumbar vertebra. Bar=1 mm. Inset: Infiltration of tumor cells was also severe under the periosteum (arrow). Bar=100 μm.
Fig. 4. Severe interstitial infiltration of tumor cells in the skeletal muscle tissue. Intracytoplasmic infiltration is also seen (arrowhead). Bar=50 μm.
Fig. 5. High magnification of interstitial infiltration of tumor cells into the skeletal muscle tissue. Bar=20 μm.
Fig. 6. Many tumor cells show severe infiltration in lymph node and invade adjacent adipose tissue. Bar=500 μm.
Fig. 7. Tumor cells diffusely infiltrate the spleen, and the normal architecture is completely lost. Bar=50 μm.
Fig. 8. Tumor cells are observed in the sinusoid and accumulate in the periportal area. Bar=100 μm.
Fig. 9. Tumor cells diffusely infiltrate the pancreas. Bar=100 μm.
Fig. 10. Tumor cells diffusely infiltrate the cortex of the kidney. Bar=100 μm.

multiple white to gray nodules up to 3 mm in size encompassing the thoracic and abdominal aorta. These nodules had a bead-like appearance near the thoracic and lumber vertebrae (Fig. 1). Most iliac lymph nodes were enlarged, up to 5 mm in diameter, in many cases; however, the borders of the lymph nodes and surrounding adipose

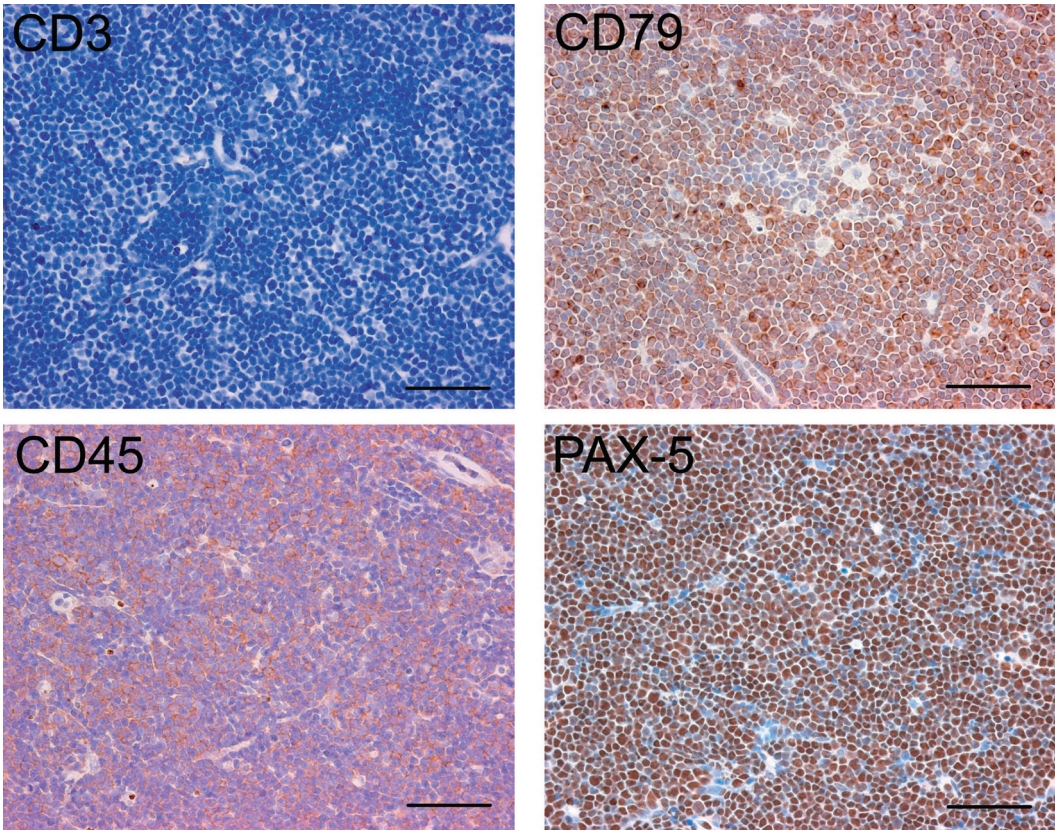

Fig. 11. Tumor cells were negative for CD3, a T-cell marker, and positive for B-cell markers PAX-5, CD79α and CD45. Bar=50 μm.

Table 1. Histopathological Examination of Malignant Lymphomas in WBN/Kob Rats

Tissue	Histopathological examination	Positive findings (%)
Spleen	Tumor cells replaced entire part of spleen	11/13 (84.6%)
Liver	Tumor cells in periportal area and sinusoids	12/13 (92.3%)
	Tumor cells in only sinusoids	1/13 (7.7%)
Submandibular lymph node	Tumor cells replaced entire part of lymph node	12/13 (92.3%)
Iliac lymph node	Tumor cells replaced entire part of lymph node	13/13 (100%)
Pancreas	Interstitial infiltration	10/13 (76.9%)
Kidney	Tumor cells in the adipose tissue of the renal hilus	12/13 (92.3%)
	Interstitial infiltration	11/13 (84.6%)
Adrenal	Tumor cells in sinusoids	9/13 (69.2%)
Lung	Interstitial infiltration	7/13 (53.8%)
Bone marrow	Tumor cells have replaced the hematopoietic cells	13/13 (100%)
Thoracic / lumbar vertebra	Tumor cells in adjacent skeltal muscle and periosteal tissue	13/13 (100%)

tissue were unclear, especially in the abdominal cavity.

Histopathology

Microscopic examination of peripheral blood smears revealed that tumor cells had scanty basophilic cytoplasm, cleaved round nuclei with fine to clumped chromatin and usually one prominent nucleolus (Fig. 2). The tumor cells were predominantly small to intermediate in size, and their morphologic characters were similar to those of mature lymphocytes.

Histopathologically, tumor cells aggregated not only in the bone marrow, spleen, lymph nodes, other lymphoid tissue and intravascular spaces of the various tissues but also in the interstitial and parenchymal tissues of many organs and tissues (Table 1). Among the various organs and tissues affected by infiltration and proliferation of tumor cells, the most characteristic and common changes were seen in the periosteal tissue and skeletal muscle adjacent to the thoracic

and lumbar vertebrae, and femur (Fig. 3). While tumor cells displaced entire parts of the marrow tissue of each bone, small numbers of megakaryocytes, erythroblastic cells and myeloblastic cells were scattered among the tumor cells. Infiltration of tumor cells was also severe under the periosteum and resulted in dissociation of these tissues, and this was often associated with partial osteolysis.

Skeletal muscle fibers and adipose tissue closely adjacent to periosteum were also entirely replaced by tumor cells. Intracytoplasmic and interstitial infiltration was evident in this area of skeletal muscle tissue (Figs. 4 and 5). Tumor cells infiltrated epidurally in the thoracic and lumber spinal cord, but central and peripheral nervous tissues, including spinal ganglions, were intact in these areas. However, tumor cells diffusely infiltrated into the trigeminal ganglia and meningeal tissue at the base of the brain in one case.

In many of the rats, enlarged lymph nodes of many rats were diffusely infiltrated by a large number of tumor cells, and normal structures such as follicles, sinues and medullary cords had completely disappeared (Fig. 6). Tumor cells frequently invaded capsules and adjacent adipose tissue (Fig. 6).

In two cases with a severely enlarged spleen, the normal architecture was completely lost, because a large number of tumor cells had proliferated in the periarterial lymphoid sheath, germinal center and red pulps with no distinct border. The location of the periarterial lymphoid sheath was estimated from the central arteries, but germinal centers and marginal zones were not distinct because of the mixed cell population of small lymphocytes and proliferated tumor cells (Fig. 7). A fairly large number of extramedullary hematopoietic cells such as megakaryocytes, erythroblastic and granuloblastic cells were observed among the tumor cells in the red pulp. The remaining 11 cases did not show any obvious enlargement, but tumor cells infiltrated diffusely in white and red pulps in 9 cases. However, in two of these eleven cases, the structures of the white and red pulps remained intact, and tumor cells were indistinguishable from hematopoietic cells or lymphocytes on sections stained with hematoxylin and eosin, even in the cases with prominent tumor cell infiltration in the liver and other tissue.

In the liver, tumor cells were most frequently observed in the sinusoid (Fig. 8). The cords of hepatocytes were atrophic in the cases with severe infiltration and proliferation of tumor cells in the sinusoid. Tumor cells also accumulated in the periportal area and formed a large mass occupying several lobules by fusion of the tumor mass in another case. Other tissues and organs involved in infiltration or proliferation of tumor cells included the pancreas, kidneys, adipose tissue of the renal hilus, adrenals, peritoneum, heart and lungs (Figs. 9 and 10). Almost all tumor cells were positive for B-cell markers, PAX-5, CD79α and CD45 and were negative for CD3, one of the T-cell markers (Fig. 11). From the results of immunohistochemistry and morphological examination, these tumors were diagnosed as malignant B-cell lymphomas.

Discussion

Lymphoma and lymphocytic leukemia have been reported in several rat strains[3–7]. According to these reports, the vast majority of spontaneous lymphomas and lymphatic leukemias have appeared in relatively aged rats[3–7]. The increased incidences of lymphomas have been induced by exposure to some chemicals in rats[17–19]. The age of onset of the disease is high except for carcinogen treatment cases[17–19]. Early onset and rapid progression of the disease is one of the characteristics of the present cases, because the average age at onset of malignant lymphoma in the WBN/Kob rats was about 60 weeks and the earliest age at onset was 35 weeks. With the exception of the sporadic cases of malignant lymphoma in various strains of rat, lymphoblastic leukemia in Sprague-Dawley rats under one year of age and T cell lymphoma in 7.5-month-old Long-Evans rats with similar infiltrative patterns into thoracic and lumber vertebrae have been reported as a lymphoproliferative disease with onset at relatively young age[1,20]. In the present case, the younger age of the affected rats and the growth pattern of the tumor cells were similar to those observed in Long-Evans rats, but the tumor cells were of B cell origin.

Among the various lymphocytic leukemias in rats, the histopathologic features of LGL leukemia (also called mononuclear cell leukemia) in F344 rats have been repeatedly described because of their frequent usage in routine carcinogenicity studies. In this type of leukemia, the spleen is the primary organ of tumor proliferation, and the bone marrow remains intact even in the late stage despite the leukemia, although tumor cells infiltrate other organs such as the liver, lungs, lymph nodes, kidneys, brain and adrenals[21]. In other types of lymphatic leukemia, infiltration into the tumor cells with spleen, liver, lymph nodes and bone marrow is common, but the involvement of other organs is not a constant feature[20–23]. The most characteristic histopathologic feature of the malignant lymphoma in the WBN/Kob rats was the leukemic pattern of neoplastic proliferation suggested by the involvement of systemic bone marrow and severe infiltration of tumor cells in mesenchymal tissue such as the adipose, periosteal and skeletal muscle tissue. This proliferating and infiltrating pattern is uncommon in other types of malignant lymphoma, including LGL leukemia. The characteristic clinical signs of the affected animals were abnormal gait with hind limb paralysis. It is well known that hind limb paralysis in laboratory animals is unusual but not a specific clinical sign of a disease that has been associated with dysfunction of the skeletal muscle and nerve systems, or infections caused by viruses and bacteria[24,25]. However, abnormal gait of the hind limb associated with lymphoma is rarely reported. Five rat and mouse cases have been reported in which spontaneous lymphoma or leukemia (Sprague-Dawley rats, NOD/LtSz-Rag1^{null} mice, Swiss Webster mice and Long-Evans rat) resulted in acute paraplegia[1,7,20,26,27], but the true cause of the

clinical signs has not been clarified. Hind limb paralysis might have been caused by direct damage to the skeletal muscle in the present cases because the spinal cords and peripheral nervous system were intact in all cases.

References

1. Nagamine CM, Jackson CN, Beck KA, Marini RP, Fox JG, and Nambiar PR. Acute paraplegia in a young adult long-evans rat resulting from T-cell lymphoma. Contemp Top Lab Anim Sci. **44**: 53–56. 2005.
2. Hayashi S, Nonoyama T, and Miyajima H. Spontaneous nonthymic T cell lymphomas in young Wistar rats. Vet Pathol. **26**: 326–332. 1989.
3. Boorman GA, Morgan KT, and Uriah LC. Spleen, lymph nodes, and thymus. In: Pathology of Fischer Rat. GA Boorman, SL Eustis, MR Elwell, J Montgomery, and WF MacKenzie (eds). Academic Press, Inc., Sandiego, California. 369–393. 1990.
4. Abbott DP, Prentice DE, and Cherry CP. Mononuclear cell leukemia in aged Sprague-Dawley rats. Vet Pathol. **20**: 434–439. 1983.
5. Gross L and Dreyfuss Y. Spontaneous tumors in Sprague-Dawley and Long-Evans rats and in their F1 hybrids: carcinogenic effect of total-body x-irradiation. Proc Natl Acad Sci USA. **76**: 5910–5913. 1979.
6. Otova B, Sladka M, Damoiseaux J, Panczak A, Mandys V, and Marinov I. Relevant animal model of human lymphoblastic leukaemia/lymphoma—spontaneous T-cell lymphomas in an inbred Sprague-Dawley rat strain (SD/Cub). Folia Biol (Praha). **48**: 213–226. 2002.
7. Richter CB, Estes PC, and Tennant RW. Spontaneous stem cell leukemia in young Sprague-Dawley rats. Lab Invest. **26**: 419–428. 1972.
8. Frith CH. Morphologic classification and incidence of hematopoietic neoplasms in the Sprague-Dawley rat. Toxicol Pathol. **16**: 451–457. 1988.
9. Frith CH, Ward JM, and Chandra M. The morphology, immunohistochemistry, and incidence of hematopoietic neoplasms in mice and rats. Toxicol Pathol. **21**: 206–218. 1993.
10. Nakama K, Shichinohe K, Kobayashi K, Naito K, Uchida O, Yasuhara K, and Tobe M. Spontaneous diabetes-like syndrome in WBN/KOB rats. Acta Diabetol Lat. **22**: 335–342. 1985.
11. Tsuchitani M, Saegusa T, Narama I, Nishikawa T, and Gonda T. A new diabetic strain of rat (WBN/Kob). Lab Anim. **19**: 200–207. 1985.
12. Narama I and Kino I. Peripheral motor neuropathy in spontaneously diabetic WBN/Kob rats: a morphometric and electron microscopic study. Acta Neuropathol. **79**: 52–60. 1989.
13. Tago Y, Katsuta O, Tsuchitani M, Narama I, and Itakura C. Glomerular lesions in spontaneously occurring diabetic WBN/Kob rats. J Comp Pathol. **104**: 367–377. 1991.
14. Ozaki K, Miura K, Tsuchitani M, and Narama I. Peripheral neuropathy in the spontaneously diabetic WBN/Kob rat. Acta Neuropathol. **92**: 603–607. 1996.
15. Matsuura T, Horikiri K, Ozaki K, and Narama I. Proliferative retinal changes in diabetic rats (WBN/Kob). Lab Anim Sci. **49**: 565–569. 1999.
16. Ozaki K, Matsuura T, and Narama I. Histochemical and morphometrical analysis of skeletal muscle in spontaneous diabetic WBN/Kob rat. Acta Neuropathol. **102**: 264–270. 2001.
17. Koestner AW, Ruecker FA, and Koestner A. Morphology and pathogenesis of tumors of the thymus and stomach in Sprague-Dawley rats following intragastric administration of methyl nitrosourea (MNU). Int J Cancer. **20**: 418–426. 1977.
18. Ogiu T, Sakura Y, and Maekawa A. Sequential observations of thymic lymphoma development induced in 10-week-old F344 rats by N-propyl-N-nitrosourea. Acta Pathol Jpn. **35**: 1191–1200. 1985.
19. Fujii E, Kimura K, Mizoguchi K, Kato A, Takanashi H, Itoh Z, Omura S, and Suzuki M. Assessment of the carcinogenic potential of mitemcinal (GM-611): increased incidence of malignant lymphoma in a rat carcinogenicity study. Toxicol Appl Pharmacol. **228**: 1–7. 2008.
20. Svoboda T, Jiricka Z, and Klir P. Spontaneous acute lymphoblastic leukemia in Sprague-Dawley rats. II. Clinicopathologic observations. Neoplasma. **36**: 149–154. 1989.
21. International classification of rodent tumours. Part I—The rat. 4. Haematopoietic system. IARC Sci Publ. 1–27. 1993.
22. Ogiu T. T-cell Lymphoma, thymic origin, rat. In: Hematopoietic System. TC Jones, JM Ward, U Mohr and RD Hunt (eds). Springer-Verlag, Berlin. 1990.
23. Frith CH, Ward JM, Brown RH, Tyler RD, Chandra M, and Stromberg PC. Proliferative lesions of hematopoietic and lymphatic systems in rats. STP/ARP/AFIP, Washington, DC. 1996.
24. Baker DG. Natural pathogens of laboratory mice, rats, and rabbits and their effects on reserch. Clin Microbiol Rev. **11**: 231–266. 1998.
25. Committee on Infectious Diseases of Mice and Rats IoLAR, Commission on Life Sciences, National Research Council. Infectious Diseases of Mice and Rats. NATIONAL ACADEMY PRESS, Washington, D.C. 1991.
26. Ceccarelli AV and Rozengurt N. Outbreak of hind limb paralysis in young CFW Swiss Webster mice. Comp Med. **52**: 171–175. 2002.
27. Shultz LD, Lang PA, Christianson SW, Gott B, Lyons B, Umeda S, Leiter E, Hesselton R, Wagar EJ, Leif JH, Kollet O, Lapidot T, and Greiner DL. NOD/LtSz-Rag1null mice: an immunodeficient and radioresistant model for engraftment of human hematolymphoid cells, HIV infection, and adoptive transfer of NOD mouse diabetogenic T cells. J Immunol. **164**: 2496–2507. 2000.